



Chemical characteristics of PM_{2.5} and organic aerosol source analysis during cold front episodes in Hong Kong, China

Yun-Chun Li ^{a,b,*}, Jian Zhen Yu ^a, Steven Sai Hang Ho ^{a,c}, Zibing Yuan ^{d,e}, Alexis K.H. Lau ^{d,e}, Xiao-Feng Huang ^a

^a Department of Chemistry, The Hong Kong University of Science and Technology, Clear Water Bay, Hong Kong, China

^b College of Life and Basic Sciences, Sichuan Agricultural University, Sichuan Province, 625014, China

^c SKLLQG, Institute of Earth Environment, Chinese Academy of Sciences, Xi'an, 710075, China

^d Atmospheric Research Center, HKUST Fok Ying Tung Graduate School, Nansha IT Park, Nansha, Guangzhou 511458, China

^e Environmental Central Facility, The Hong Kong University of Science and Technology, Clear Water Bay, Hong Kong, China

ARTICLE INFO

Article history:

Received 11 January 2012

Received in revised form 30 May 2012

Accepted 31 May 2012

Available online 8 June 2012

Keywords:

Fine organic carbon

Source apportionment

Chemical mass balance

Organic tracers

Episode

Secondary organic aerosol

ABSTRACT

In this study, we investigate the influence of long-range transport (LRT) episodes brought in by cold front on the concentration levels of PM_{2.5}, major aerosol constituents, organic tracers, and PM_{2.5} source characteristics in Hong Kong, China. PM_{2.5} samples were collected during January–March 2004 and January–March 2005 and analyzed for major constituents and organic tracer species. Synoptic weather conditions and characteristics of common air pollutants were used to categorize the sampling days to three groups, i.e., groups mainly affected by local emissions or regional transport (RT) or cold front LRT. Concentrations of PM_{2.5} mass and its major constituents during cold-front days were lower than those during RT-dominated periods but higher than those during local emissions-dominated periods. Source apportionment using chemical mass balance (CMB) indicates that vehicular exhaust was a significant primary OC source of mainly local emissions, making average contributions of 1.82, 1.50, and 2.39 $\mu\text{g C m}^{-3}$ to OC in the local, LRT, and RT sample groups, respectively. During cold front periods, primary OC concentrations attributable to biomass burning and coal combustion were approximately triple and double, respectively, those during periods dominated by local emissions. Suspended dust, a minor primary OC source (0.24–0.40 $\mu\text{g C m}^{-3}$), also showed increased contribution during cold fronts. The unexplained OC by CMB (i.e., total OC minus apportioned primary OC), an approximate indicator for secondary OC, was a significant fraction of OC (>48%) and its mass concentration was much higher in the cold front LRT and RT sample groups (6.37 and 9.48 $\mu\text{g C m}^{-3}$) than in the local sample group (3.8 $\mu\text{g C m}^{-3}$). Source analysis as well as tracer concentration variation shows that biomass burning OC and water soluble organic carbon (WSOC) were correlated, suggesting biomass burning as a significant contributor to WSOC.

© 2012 Elsevier B.V. All rights reserved.

1. Introduction

Suspended particulate matter (PM) is the most important pollutant contributing to air pollution in China, especially in

economically rapid-growing area such as the Pearl River Delta (PRD) region. The overall epidemiologic evidence suggests that particulate air pollution, especially fine combustion-source pollution common to many urban and industrial environments, is an important risk factor for cardiopulmonary disease and mortality (Pope, 2000a, 2000b). Many studies also suggested that exposure to high levels of fine PM during episodic events are associated with adverse health effects among sensitive subgroups (Peters et al., 2000; Schwartz et al., 1996).

* Corresponding author at: College of Life and Basic Sciences, Sichuan Agricultural University, Sichuan Province, 625014, China Tel.: +86 835 2886179; fax: +86 835 2886136.

E-mail address: yunchunli@sicau.edu.cn (Y.-C. Li).

The Hong Kong Environmental Protection Department (HKEPD) has implemented a regular monitoring program for total suspended particulates and respirable suspended particulates (RSP) since the mid 1980s, which gathers aerosol samples once every six days for detailed chemical compositional analyses. A number of studies have used data based on the regular one-in-six day sampling schedule to investigate seasonal and spatial variations, undertake source apportionment, and examine the relative importance of local emissions versus regional transport (Ho et al., 2006; Louie et al., 2005; Yuan et al., 2006; Zheng et al., 2006). The HKEPD monitoring program was designed mainly to monitor average concentrations. As a result, it was not very useful for understanding of episodic events, which typically last for about one to three days. There were a few studies reporting investigations of episodic events influencing air quality in Hong Kong (Fang et al., 1999; Fung et al., 2005; Lee and Hills, 2003; Wai and Tanner, 2005; Wang et al., 2006). Fang et al. (1999) reported a dust episode associated with LRT from northern China during 9–10 May 1996. Much higher concentrations of Al, Fe, and Ca were observed during this episode. Fung et al. (2005) reported an air pollution episode caused by biomass burning in the northeast part of the PRD, as indicated by high concentration of potassium ions during this period. Liu and Chan (2002) examined the relationship between the winter episodes and boundary layer dynamics and land–sea breezes in 1999. Lee and Hills (2003) analyzed pollution episodes in Hong Kong during 1996–2002 and concluded that episodic conditions in winter were usually associated with protracted weak northeast monsoon conditions while episodes in the spring season were traceable to long-range transport (LRT) dust storm events originating in deserts in the north or northwestern China. Wai and Tanner (2005) suggested that the LRT contributions were significant and account for ~66% of the PM₁₀ episode days during 1998–2001.

The HKEPD monitoring program did not include detailed speciation work to a molecular level for the organic carbon (OC) fraction. Only a few studies have reported chemical characterization of the OC fraction and source apportioning of organic aerosol. Zheng et al. (2006) investigated the composition and sources of fine carbonaceous aerosols in Hong Kong with chemical mass balance (CMB) model based on individual organic tracer information collected from a 12-month ad hoc project in 2000–2001. To our best knowledge, there is a lack of work on chemical characterization of the OC fraction and source apportionment during PM episodic periods in Hong Kong.

In this study, we target to study PM_{2.5} (particulate matter of aerodynamic diameter less than 2.5 μm) aerosol characteristics and major OC sources during cold front episodes in Hong Kong. PM_{2.5} samples were collected at Yuen Long (YL) station during January–March 2004 and January–March 2005. High-volume sampling was activated by cold front episodic forecast. The aims of this study are (1) to obtain chemical characteristics of fine aerosol during cold front episodes, including major constituents and individual organic species; (2) to identify the major sources of fine OC; and (3) to investigate the effect of cold front episodes on PM_{2.5} mass, its major compositions and major OC contributing sources in Hong Kong.

2. Methods

2.1. Sampling

Samples were collected at Yuen Long (YL), located in the northwestern corner. It is an air quality monitoring station where long-term air quality and meteorological measurements are available through the monitoring efforts by HKEPD. As a result of regional land–sea circulation being located more in the western side of the Pearl River Estuary, YL station, from time to time, has the highest PM₁₀ (particulate matter with aerodynamic diameters of <10 μm) concentrations among all the air quality monitor stations in Hong Kong (Lo et al., 2006). The sampling site is 25 m above the ground and located on the rooftop of a building. Sampling of cold front-influenced air was activated by episodic forecast during January–March 2004 and January–March 2005. Each 24-h PM_{2.5} sample was collected on a quartz filter (20×25 cm, prebaked at 550 °C for at least 8 h) using a high-volume air sampler (GT22001; Andersen Instruments, Smyrna, GA, USA) at a flow rate of 1.13 m³ min⁻¹. A total of 21 samples were collected. The filter samples were stored in a freezer at 4 °C until analysis.

2.2. Chemical analysis

A filter punch of 1×1 cm² in size from each filter was removed for elemental carbon (EC) and OC analysis using a thermal/optical aerosol carbon analyzer (Sunset Laboratory, Forest Grove, OR, USA). The thermal analysis conditions were the same as those established for the NIOSH method 5040 for diesel particulate (Birch and Cary, 1996). Duplicate measurements of OC and EC were made on every sample, and the average relative standard deviations (RSD) were 4% and 9% for OC and EC, respectively (Yang et al., 2005). The water-soluble organic carbon (WSOC) content was determined by measuring the OC content in the aerosol water extracts using a total organic carbon (TOC) analyzer (Model TOC-5000A, Shimadzu, Kyoto, Japan) (Yang et al., 2003). A circular punch of 4.7 cm in diameter was extracted with 10 mL aliquots of UV-oxidized high-purity water in a sonication bath for 30 min. The water extracts were rid of filter debris and suspending insoluble particles using a syringe filter. A 3-mL aliquot of the extract was used for quantification of carbon content with the TOC analyzer, and the RSD of multiple consecutive measurements for six aerosol samples were <3% (Yang et al., 2003). The remaining water extracts were used for analysis of organic anions (i.e., formate, acetate, methanesulfonate, oxalate), inorganic anions (i.e., Cl⁻, NO₃⁻, and SO₄²⁻) and cations (i.e., NH₄⁺, K⁺, Na⁺, Ca²⁺, and Mg²⁺) using an ion chromatography (IC) system (DX500, Dionex, Sunnyvale, CA) (Yang et al., 2005). The recoveries of the target ions spiked into duplicated blank filter were in the range of 92–108%.

Two filter strips of 1×1.45 cm² in size were cut for the quantification of non-polar organic compounds (including n-alkanes, branched alkanes, polycyclic aromatic hydrocarbons (PAHs), and hopanes) using in-injection port thermal desorption (TD) and subsequent gas chromatography–mass spectrometry (GC-MS) (GC6890/MS 5973, Agilent, Santa Clara, CA, USA) analysis method (Ho and Yu, 2004). The minimum detection limits (MDLs) in nanograms per sample were in the range of 0.08–1.64 ng for alkanes, 0.22–2.28 ng for PAHs and 0.15–0.68 ng for hopanes. Replicate analyses were conducted on

every 10th sample. The RSDs for the samples were <6.0% for targeted compounds (Ho et al., 2008, 2011). One-quarter of the 20×25 cm² quartz filter was used for analysis of 15 sugar compounds (i.e., monosaccharides, sugar alcohols, anhydrosugars, and disaccharides) with solvent extraction followed by silylation with *N,O*-bis(trimethylsilyl)trifluoroacetamide (BSTFA) and GC-MS detection (Medeiros and Simoneit, 2007; Simoneit et al., 2004). Recoveries of the targeted sugars were >70%. The reproducibility errors of the methods for the determination of organic species was <15%. The analysis of mono- and dicarboxylic acids, ω-oxo-carboxylic acids, mid-chain ketocarboxylic acids, and aldehydes were carried out using a method developed in our laboratory (Li and Yu, 2005). Briefly, one-fourth of the 20×25 cm² quartz filter was mixed with a mixture of boron trifluoride (BF₃)/butanol (BuOH) for derivatization. The reaction mixture was washed with water. The derivatives in the hexane layer were separated from the mixture and injected into the GC-MS system for analysis. The recoveries of eight deuterated internal standards spiked into an aerosol loaded filter sample were in the range of 96.8–105.3% (except phthalic acid–D₄ was 53%). The target analytes had their MDLs in the range of 0.06–1.8 ng/μL.

Trace elements were quantified by inductively coupled-plasma atomic emission spectrometry (ICP-AES). A circular punch of 4.7 cm diameter in size was cut and underwent microwave-assisted digestion with HNO₃/H₂O₂ added as the digestion reagent (Swami et al., 2001). Due to the limited sensitivity of ICP-AES, only abundant elements were quantified, including Al, Ba, Ca, Cu, Fe, K, Mg, Mn, Na, Pb, V and Zn. The recoveries of the target elements were in the range of 61–92%, with SD<9%, except for Al and K (SD>20%). In comparison with the IC method, the extent of agreement for the cation species (i.e., K⁺, Mg²⁺, and Ca²⁺) in the 21 aerosol samples was assessed as a simple linear fit (Figure S1) (hereafter, Figure S# and Table S# denotes materials provided as supporting information). Good agreements between the two methods were indicated by coefficient of determination (*R*²) values in

the range of 0.90–0.99 (*n* = 21) and slope values in the range of 0.89–1.26.

3. Results and discussion

3.1. Synoptic analysis

Synoptic weather conditions (i.e., temperature, relative humidity (RH), wind speed and direction) and main air quality parameters (i.e., air pollution index (API), RSP, SO₂, CO, O₃) were obtained from Environmental Central Facility at the Hong Kong University of Science & Technology (<http://envf.ust.hk/>) and time resolution is 1 h. The meteorological and criteria air pollutant data were examined for individual sampling days in the two sampling periods (11 January–3 March, 2004 and 31 January–17 March, 2005) (Figures S2–S5) and used to categorize the 21 samples into local emissions-, regional transport (RT)-, and cold front LRT-influenced samples. Fig. 1 plot the temperature, wind speed and direction variations at YL during the two sampling periods. The classifications of individual samples are listed in Table 1. Samples collected on days under dominant influence of emissions local to Hong Kong are referred as local samples. Samples collected on days of significant regional influence from the PRD are referred as RT samples. Samples collected on cold front days are referred LRT samples, as cold fronts bring in air outside the PRD. The wind direction associated with cold front is very often northerly or northeasterly, bringing pollutants from northern and eastern China along the coastline to Hong Kong. It should be noted that even during RT or LRT-influenced periods, there was significant mixing of outside air with locally generated pollutants.

3.1.1. Cold front episodes

Cold front periods were identified by significant drops in ambient temperature and concurrent increase in wind speed. There were seven cold front episode samples during our sampling periods. They were 040113, 040117, 040121, 040203,

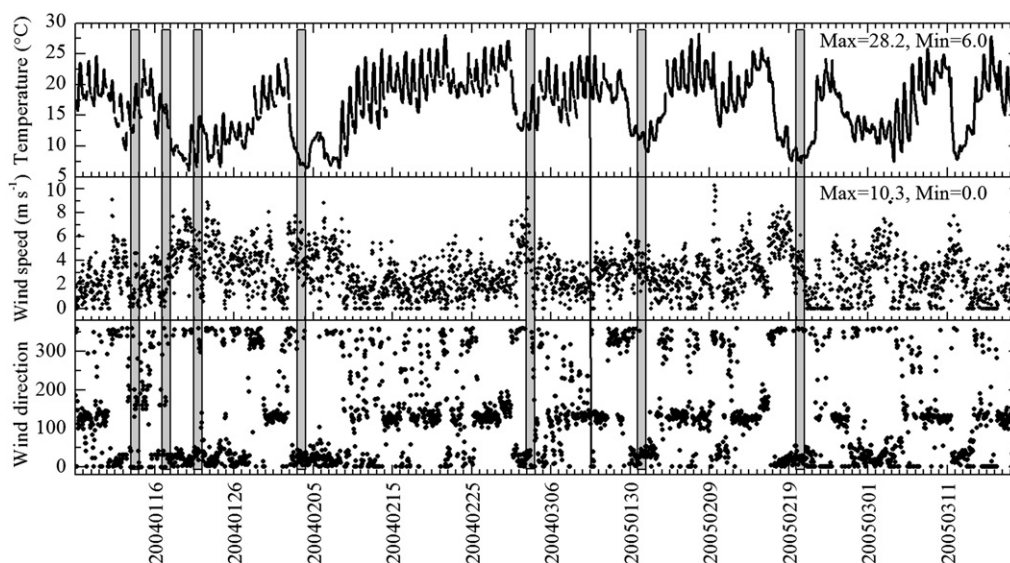


Fig. 1. Variations of temperature, wind speed and direction at YL station during sampling periods. (Linear line separate between Mar. 10, 2004 and Jan. 25, 2005; shaded areas are cold front-LRT samples).

Table 1Concentrations ($\mu\text{g m}^{-3}$) of major components in $\text{PM}_{2.5}$, OC/EC, and K^+ /EC ratios during different episodic conditions.

Sample ID ^a	$\text{PM}_{2.5}$	OC	EC	SO_4^{2-}	NO_3^-	Cl^-	Na^+	NH_4^+	K^+	Mg^{2+}	Ca^{2+}	Others ^b	WSOC	OC/EC	K^+ /EC
<i>Local emissions-dominated samples</i>															
040115	39.53	9.02	3.01	10.83	1.48	0.32	0.48	7.50	0.45	0.07	0.17	0.79	3.20	3.00	0.15
040131	39.92	6.62	2.40	10.46	2.87	0.35	0.35	7.80	0.46	0.05	0.13	4.45	2.47	2.75	0.19
040221	32.88	7.54	3.73	8.50	1.92	1.19	0.38	8.94	0.26	0.04	0.07	-4.23	2.22	2.02	0.07
040229	21.87	3.20	2.21	7.08	0.23	0.00	0.34	5.68	0.20	0.04	0.05	0.92	1.56	1.44	0.09
040301	44.30	8.14	3.21	7.88	1.88	1.00	0.22	6.19	0.56	0.03	0.11	10.20	2.21	2.54	0.17
050228	24.03	7.30	2.79	3.83	2.43	0.26	0.09	4.49	0.42	0.01	0.06	-2.02	2.54	2.61	0.15
050317	47.77	11.93	3.92	7.87	4.02	0.35	0.22	8.12	0.41	0.03	0.08	3.67	4.05	3.04	0.10
Avg.	35.76	7.68	3.04	8.07	2.12	0.58	0.30	6.96	0.39	0.04	0.10	1.97	2.61	2.49	0.13
<i>Samples influenced by cold front-long range transport</i>															
040113	58.40	14.43	2.16	16.41	4.32	0.46	0.13	10.44	1.07	0.02	0.18	0.11	6.24	6.68	0.50
040117	41.55	9.51	1.65	10.11	3.82	0.47	0.24	8.33	0.58	0.14	0.07	0.91	4.46	5.75	0.35
040121	53.0	12.98	1.83	14.46	4.86	0.31	0.17	9.39	2.10	0.13	0.20	-1.25	6.84	7.08	1.14
040203	34.08	8.43	2.24	7.01	3.10	0.97	0.12	6.95	0.55	0.01	0.07	-0.44	2.53	3.77	0.25
040303	44.66	9.23	2.55	11.48	1.61	0.22	0.20	7.94	1.11	0.05	0.26	4.47	3.73	3.63	0.44
050131	45.41	12.21	2.39	10.19	6.91	1.13	0.12	9.15	0.92	0.02	0.08	-5.03	4.87	5.11	0.39
050220	78.20	14.90	2.76	23.13	5.87	0.97	0.21	13.48	1.33	0.07	0.17	6.37	7.32	5.40	0.48
Avg.	50.75	11.67	2.23	13.26	4.36	0.65	0.17	9.38	1.10	0.06	0.15	0.73	5.14	5.34	0.51
<i>Samples influenced by regional transport from PRD</i>															
040111	48.70	14.90	2.51	10.94	5.00	0.27	0.25	8.62	1.04	0.03	0.17	-3.98	4.54	5.93	0.42
040116	44.43	12.05	3.33	7.70	3.70	0.61	0.16	9.18	1.54	0.04	0.20	-1.30	5.00	3.62	0.46
040130	136.8	25.03	5.90	25.26	17.81	2.20	0.46	21.89	2.60	0.09	0.22	20.33	11.12	4.24	0.44
040222	76.44	19.20	2.84	17.63	3.07	0.27	0.44	11.08	1.56	0.07	0.18	8.59	9.61	6.76	0.55
050204	54.11	11.59	3.88	12.29	5.89	1.35	0.20	10.08	0.38	0.02	0.07	1.39	3.98	2.98	0.10
050222	63.71	16.95	5.21	15.82	7.22	2.04	0.23	11.72	0.89	0.02	0.07	-6.60	5.67	3.25	0.17
050305	64.90	16.22	4.06	17.16	4.69	0.61	0.27	10.01	1.18	0.07	0.27	0.63	6.96	3.99	0.29
Avg.	69.87	16.56	3.96	15.26	6.77	1.05	0.29	11.80	1.31	0.05	0.17	2.72	6.70	4.40	0.35

^a The sample ID is sampling date in yymmdd.^b "Others" is the residue mass, i.e., the mass difference between $\text{PM}_{2.5}$ mass and the sum of the major constituents, $\text{OM} = 1.6 * \text{OC}$.

040303, 050131, and 050220 (the sample names coded in the format of yymmdd). During each cold front episode, temperature decreased significantly, wind speed increased to higher than 4 m s^{-1} and wind direction changed to northerly/northeasterly (Fig. 1). For example, the temperature decreased from 18.5°C to 6°C during the cold front occurred in 17–21 January 2004 and from 24.3°C to 6.4°C during the 2–4 February 2004 cold front. Strong northeasterly wind with an average wind speed of 5.1 m s^{-1} was recorded at Tap Shek Kok wind station on 3 February. Temperature and wind conditions of other cold fronts were similar and illustrated in Figure S2. Back trajectories of air masses on these days (Figure S6) illustrate that the origin of air masses during these cold fronts were from Southeastern China (mainly from Jiangxi, Fujian, and Guangdong Provinces). Among them, air masses of 040113 and 040117 samples that were originated from Jiangxi Province, moved towards southeast and reached Hong Kong through the coastal areas in Southern China. Air masses influencing the other cold front samples reached Hong Kong mainly from Jiangxi Province and directly through Guangdong Province.

During the cold front periods, the criteria air pollutants (API, RSP, SO_2 , NO_2 , O_3 and CO) measured at the air quality monitoring stations covering both rural and urban locations showed similar concentration levels across Hong Kong (Figure S3). The lack of spatial variation conformed to the dominant influence of LRT. In addition, the concentrations of SO_2 were at relatively low levels, consistent with the expectation that SO_2 have been oxidized to sulfate during LRT. During all cold front episodes in this study, the difference in O_3 concentrations was

small between rural and urban sites, and high night-time/morning O_3 concentrations were typically observed. These characteristics were consistent with the observations reported by Wai and Tanner (2005) for LRT episodes.

3.1.2. Regional transport episodes

Seven sampling days were identified to be associated with synoptic weather conditions that favor regional transport of air masses. The period of 29–30 January 2004 was characterized by elevated concentrations of all major air pollutants, among which RSP, SO_2 , CO and NO_x increased to $292 \mu\text{g m}^{-3}$, 62 ppb, 2.72 ppm and 244.4 ppb, respectively, on 30 January 2004 (Figure S4). Medium northwesterly/northerly wind dominated Hong Kong, especially the western region. All the monitored air pollutants had much higher levels in the western region than in the eastern region. The highest hourly RSP concentrations were $330 \mu\text{g m}^{-3}$ in the western region and $180 \mu\text{g m}^{-3}$ in the eastern region on 30 January 2004. Elevated level in SO_2 was also a characteristic feature of region transport influence. SO_2 was at much higher levels during the RT-dominated period than during cold front LRT-influence period because SO_2 was mainly from within the PRD region and did not experience as long transport and concomitant oxidation as SO_2 transported from outside the PRD during the LRT periods. Concentrations of the pollutants started increasing at 8:00 am on 29 January 2004 in the western region while the increasing in the eastern region lagged behind and the increase started at 4:00 am on 30 January 2004 in the eastern region.

Four sampling days (040116, 040222, 050204, and 050305) were mainly affected by land–sea circulation due to weak background wind and sunny periods in the afternoon, trapping regional air pollutants in the western part of Hong Kong (Lo et al., 2006). The SO_2 concentrations on these days were higher than 7.64 ppb, which is a typical local emission-affected SO_2 level (Lau et al., 2007). For example, SO_2 concentration of 040222 reached 83 ppb in the afternoon.

Sample 040111 was collected at the beginning of a cold front when the PRD air mass was brought to Hong Kong and accumulated. Sample 050222 was collected immediately after a cold front. Weak northeasterly wind brought Shenzhen air pollutants to Hong Kong, accompanied with increased SO_2 concentration. Wai and Tanner (2005) examined 4-year (1998–2001) air quality data in Hong Kong and differentiated RT and cold front days using certain characteristics of O_3 . They observed that O_3 concentrations were very low at urban locations but high in rural areas during regional episodes and that only small difference in O_3 concentrations existed between rural and urban sites during LRT episodes. At the same time, there were afternoon peaks of O_3 during regional episodes while higher O_3 concentrations in night-time/morning during LRT episodes. For the 040111 and 050222 samples, O_3 had much higher concentrations at the rural sites and relatively low values at the urban sites. There were afternoon peaks of O_3 , consistent with the conclusions of regional episodes by Wai and Tanner (2005).

3.1.3. Samples dominated by local emissions

Seven sampling periods were identified to be dominated by local emissions. Samples 040115, 040131, 040221, 040229, and 040301 were mainly affected by southerly/southeasterly/easterly wind, which brought clean marine air mass to Hong Kong. Under such conditions, local emissions were the dominant sources of PM. There were no significant variations in the concentrations of RSP, SO_2 , NO_2 , CO and O_3 at most air quality stations across Hong Kong (Figure S5). RSP and SO_2 were generally at very low levels across Hong Kong while O_3 was at higher levels due to lower NO titration effect.

Sample 050317 were identified to be mainly affected by local vehicle/marine according to the spatial pattern of SO_2 . On this day, higher levels of SO_2 were observed at the monitoring stations near the city's container port (i.e., at the Kwai Chung and Shan Shui Po stations) while much lower level at YL and Tap Mun, two stations located in the northern part of Hong Kong.

Sample 050228 was also identified to be mainly local emissions-influenced on the basis of low level SO_2 in Hong Kong.

3.2. $\text{PM}_{2.5}$ mass concentrations and chemical compositions

3.2.1. Mass concentrations and major ion species

Major compositions of $\text{PM}_{2.5}$ are tabulated in Table 1 and illustrated in pie charts in Fig. 2. A factor of 1.6 was used to convert OC to organic matter (OM) mass (Turpin and Lim, 2001). OM ranged from 12.3 to $26.5 \mu\text{g m}^{-3}$. With a percentage contribution of 34.4–37.9%, OM contributed most to $\text{PM}_{2.5}$. SO_4^{2-} (8.1 – $15.3 \mu\text{g m}^{-3}$) and NH_4^+ (7.0 – $11.8 \mu\text{g m}^{-3}$) were the next two most abundant constituents, accounting for 21.8–26.1% and 16.9–19.5% of $\text{PM}_{2.5}$, respectively. NO_3^- and EC contributed 5.9–9.7% and 4.4–8.5% of $\text{PM}_{2.5}$, respectively. WSOC account for 27.1–52.7% (avg. 39.4%) of OC. Identified water-soluble organic species accounted for 18.3–43.1% (avg. 30.1%) of WSOC on a carbon mass basis.

During cold front episodes, the levels of $\text{PM}_{2.5}$, OM, SO_4^{2-} , NO_3^- , NH_4^+ , K^+ , and WSOC were between the levels in the local emissions-dominated samples and in the RT-dominated samples (Table 1). The percentage contributions of SO_4^{2-} and WSOC in $\text{PM}_{2.5}$ during cold front periods were the highest, accounting for 26.1% and 10.1%, respectively, in agreement with that secondary products were formed during LRT (Fig. 2). The most significant difference between cold front periods and local emissions-dominated periods was K^+ , which was 180% higher than that in the local influence-dominated samples. Generally speaking, EC could originate from various combustion sources; however, in Hong Kong, existing measurements point to vehicular emissions to be the dominant source. This point has been discussed in details by Lin et al. (2010). Considering that K^+ and EC are indicators of biomass burning and local vehicle exhaust, respectively, one could use the K^+/EC ratio to indicate the relative importance of the two primary PM sources. The K^+/EC ratio was an average 0.51 (range: 0.25–1.14) during the cold front periods; an average of 0.35 (range: 0.10–0.55) during RT-influenced periods, and an average of 0.13 (0.07–0.19) during local emissions-dominated periods. The much higher K^+/EC ratio during cold front periods and RT-influenced periods than that during the local emissions-dominated periods indicated that long range transported air masses from Northern China and regional air masses had more PM from biomass burning relative to vehicular emissions.

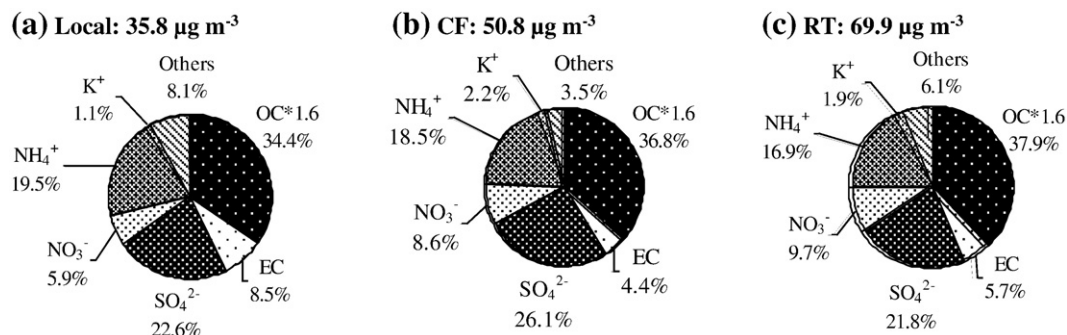


Fig. 2. Mass and major compositions of $\text{PM}_{2.5}$ at YL station during different episodic periods. (a) Local emissions-dominated sample group, (b) cold front LRT-influenced sample group, and (c) regional transport (RT)-influenced sample group.

3.2.2. OC, EC, and WSOC

OC showed significant variations among the three different synoptic weather conditions, with 7.7, 11.7, and 16.6 $\mu\text{g C m}^{-3}$ during local, cold front, and RT periods, respectively. In comparison, the variation of EC was much smaller. This indicates that locally-emitted EC dominated at all times. The lowest EC level was seen during cold front periods. This was a combined result of faster dispersion of local pollution due to the stronger wind and the air mass transported from the north containing less EC. The OC/EC ratio has long been recognized to be an indicator of relative contribution of primary and secondary organic aerosols. The OC/EC ratio exceeding 1.8–2.75 has been used to indicate significant presence of second organic aerosols (SOA) (Gelencser, 2004). In this study, the samples collected during the cold front periods had higher OC/EC ratios (3.6–7.1), an expected result of more SOA formed during LRT as well as the deposition of EC during the transport. In comparison, the samples collected during local emissions-dominated periods had lower OC/EC ratios (1.4–3.0), reflecting the presence of more freshly-emitted aerosols. The samples collected during RT periods also had high OC/EC ratios (3.0–6.8), indicating significant presence of SOA.

WSOC was a significant fraction and accounted for 27–53% (avg. 39%) of OC in all three groups of samples, which is similar to that of semi-rural station (avg. 41%) and higher than those of urban, roadside, and rural stations (avg. 21–29%) in the PRD region (Huang et al., 2012). Local-influenced samples had the lowest fraction (35%), while cold front-influenced samples had the highest fraction (43%). WSOC was found to be positively correlated with sulfate ($R^2=0.79$, $n=21$), a finding also reported in other studies (e.g., Huang et al., 2006). The correlation with sulfate suggests that WSOC was of dominantly regional/secondary origin. The secondary nature of WSOC was also supported by the observation that samples of high WSOC concentrations generally also have high OC/EC ratios (Table 1).

3.2.3. Elements

Twelve elements were quantified using ICP-AES, including Al, Ba, Ca, Cu, Fe, K, Mg, Mn, Na, Pb, V, and Zn. Concentrations of these elements during different episodic periods are compared in Figure S7a. The concentration levels of these elements during cold front episodes were either similar to or slightly lower than those in the RT-influenced periods while the concentrations in the local samples were consistently at the lowest (Figure S7a). The concentrations of Al, Fe, and Ca in the cold front and RT-influenced samples were much higher than those in the local samples, indicating transport of dust materials to Hong Kong. The average concentrations of Al, Fe, and Ca in the cold front-influenced samples were 194, 292, and 268 ng m^{-3} , respectively, which were 1.4–1.9 times those in the local emissions-influenced samples. Dust episode from northern China by LRT with very high concentrations of Al, Fe, and Ca was reported by Fang et al. (1999).

Crustal enrichment factors (EF) were calculated to compare the composition of the ambient PM samples with the average elemental composition of earth's crust (Weast, 1988). The EF of element X_i is calculated to be $(X_i/\text{Al})_{\text{sample}}/(X_i/\text{Al})_{\text{crust}}$. Low EF values (<5.0) were found for Al, Fe, Mg, and Ca, indicating that these species in $\text{PM}_{2.5}$ were dominated by crustal material. Hagler et al. (2007) also found that Si, Ca, Sr and Fe were dominated by crustal material in Hong Kong. High EF values

(>10) were observed for Cu, K, Pb, V and Zn, consistent with their expected anthropogenic origin (Figure S7b).

The relative magnitude of EF among the three groups of samples indicates the possible sources. K and Pb had higher EF in the RT-influenced samples and cold front samples than those in the local samples. K is a biomass burning tracer and Pb is mainly from leaded gasoline and industrial emissions. This observation indicated that the PRD region and northern China have more sources of biomass burning and leaded gasoline/industrial emissions than Hong Kong. In comparison, Ba, Ca, Cu, Mg, Na, and V had higher EF during local emissions-influenced periods than RT-influenced and cold front periods. This observation means that these elements were dominated by local emissions (e.g., sea salt, ship emissions). Local Cu emissions may come from vehicular emissions (brake wear) and/or local printed circuit board manufacturing. The presence of V in Hong Kong area has been previously related to fuel oil combustion which is mainly from shipping activities (Yu et al., 2004). Our measurements were in good agreement with the study by Hagler et al. (2007).

3.2.4. Individual organic compounds

In the organic fraction, a total of 170 organic compounds in eight compound classes (n-alkanes, hopanes, PAHs, fatty acids, sugar compounds, dicarboxylic acids, ketocarboxylic acids, and dicarbonyls) had been identified and quantified. They accounted for 8.9–15.8% (avg. 12.6%) of OC on a carbon mass basis. Comparisons of select individual organic compounds in different episode samples are shown in Figure S8.

3.2.4.1. Alkanes. The total concentrations of n-alkanes (C_{15} – C_{36}) in local, cold front, and RT samples were 82, 122, and 137 ng m^{-3} , respectively (Figure S8a). The three odd n-alkanes (C_{29} , C_{31} , and C_{33} -alkanes) are tracers of vegetative detritus. Their concentration levels during the cold front periods were lower than those in the RT-influenced periods but higher than those in the local samples.

The total concentrations of C_{30} – C_{32} branched alkanes were 6.72, 6.48, and 8.25 ng m^{-3} during the local emissions-influenced, cold front, and RT-influenced periods, respectively (Figure S8b). Similar levels of the individual C_{30} – C_{32} branched alkanes were observed among the three types of samples, indicating that these compounds were mainly associated with local sources. Branched alkanes are tracers of cigarette smoke or burning of plants related to tobacco. Contribution of cigarette smoke in these $\text{PM}_{2.5}$ samples was readily identified by a predominance of odd number iso-alkanes (i.e., iso- C_{31} and iso- C_{33} more abundant than iso- C_{30} and iso- C_{32}) and even number anteiso-alkanes in the range of C_{29} – C_{33} (i.e., anteiso- C_{30} and C_{32} more abundant than anteiso- C_{31} and anteiso- C_{33}). This is because the leaf surface wax of the tobacco plants is enriched in iso-alkanes and anteiso-alkanes.

3.2.4.2. Hopanes. Hopanes are found in diesel fuel, and present in lubricating oil used by diesel-powered and gasoline-powered motor vehicles (Cass, 1998). They are molecular tracers for PM emitted from motor vehicles (Schauer et al., 1996). The total concentrations of hopanes were 7.3, 8.1, and 11.6 ng m^{-3} in the local, cold front and RT-influenced samples, respectively (Figure S8c). Similar to the branched-alkanes, hopanes were also found to have similar concentrations in

the cold front-influenced samples and the local emissions-influenced samples, indicating that hopanes were mainly derived from local emissions. Unlike branched-alkanes, the difference in hopanes concentrations between RT- and local emissions-influenced samples was obvious, which means that regional sources had some contribution to hopanes in PM_{2.5} in Hong Kong. Hopane data in this study is also consistent with other measurements in Hong Kong. Yu et al. (2011) studied a larger data set of hopanes and EC measurements in different locations from roadway tunnel, roadside to typical urban locations in Hong Kong and concluded that vehicular emissions dominated the ambient concentrations of hopanes in Hong Kong.

3.2.4.3. PAHs. PAHs are products of incomplete combustion from various sources, such as fossil fuel combustion, coal combustion, natural gas combustion and biomass burning. The total concentrations of PAHs were 8.0, 18.2 and 17.2 ng m⁻³ in the local, cold front and RT-influenced samples, respectively (Figure S8d). Unlike hopanes, PAHs were significantly higher in the RT-influenced and cold front samples than those in the local samples. Compared with the relative small variations of hopanes among different groups of samples, significant variations of PAHs suggested that there were significant regional and super-regional sources making contributions to PAHs. Biomass burning and coal combustion were likely candidates for such regional and super-regional sources, as indicated by elevated K⁺ and sulfate concentrations in the RT-influenced and cold front samples. PAH data in Yu et al. (2011) also show strong evidence of biomass burning and other regional/super-regional combustion sources dominating ambient PAH concentrations in Hong Kong. Ratio of Fluoranthene/(Fluoranthene + Pyrene) is often used to evaluate the sources, which is between 0.40 and 0.50 for petroleum combustion and >0.50 for grass, wood or coal combustion (Tan et al., 2011). In this study, the ratios were 0.49 ± 0.04, 0.52 ± 0.03 and 0.50 ± 0.04 during local, cold front and RT-influenced samples, respectively, suggesting that petroleum combustion might be the main source of PAHs in local emissions-influenced samples, while biomass and coal combustion might be the main sources in cold front and RT-influenced samples.

3.2.4.4. Fatty acids. The average concentrations of the total fatty acids (C₆–C₃₂) were 528, 894, and 1236 ng m⁻³ during the local emissions-influenced, cold front and RT-influenced periods, respectively (Figure S8e). The individual species also had the similar increasing trend from the local samples, cold front samples, to RT-influenced samples. C₁₆ was the most abundant compound in all samples, followed by C₁₈. Homologues <C₂₀ are thought to derive in part from microbial sources while homologues >C₂₂ are from vascular plant wax. Besides microbial activities, cooking has been found to be a major contributor of <C₂₀ fatty acids in urban areas. For example, 21% of the primary fine OC particle emissions in the Los Angeles area were due to meat cooking (Rogge et al., 1991). A number of other sources also produce fatty acids, such as biomass burning, vehicle exhaust, and marine aerosol. The significant increases in the concentration of fatty acids during the cold front and RT-influenced periods indicate that regional and super-regional sources had some contribution to fatty acids in Hong Kong.

3.2.4.5. Sugar compounds. Fifteen sugar compounds, including four monosaccharides (xylose, fructose, mannose and glucose), two anhydrosaccharides (galactosan and levoglucosan), six sugar alcohols (glycerol, threitol, xylitol, arabitol, mannitol and sorbitol), and three disaccharides (sucrose, maltose and mycose) were quantified (Li, 2008). The most abundant sugar compound identified in these samples was levoglucosan, with concentrations of 33, 104, and 185 ng m⁻³ in the local, cold front, and RT-influenced samples, respectively. Levoglucosan has been used as a source-specific tracer for biomass burning due to a high resistance to degradation in the atmosphere and the fact that it cannot be generated by noncombustive processes, e.g., hydrolysis or microbial degradation of carbohydrates (Gelencser, 2004). Its concentration was significantly higher during cold front and RT-influenced periods compared to the local emissions-influenced samples, consistent with the K⁺ data in showing that Hong Kong was significantly affected by biomass burning from northern China and the PRD region.

Mono- and di-saccharides and sugar alcohols were identified as part of the natural background aerosol and are suggested to be derived from airborne and soil-borne microbes and other biogenic materials (Graham et al., 2002; Simoneit et al., 2004). The total concentrations of mono- and disaccharides and sugar alcohols were 10.5, 18.2, and 31.9 ng m⁻³ in the local, cold front, and RT-influenced samples, respectively. The elevated concentrations of sugar compounds were consistent with the increased contribution from suspended soil, as indicated by the crustal elemental data.

3.2.4.6. Di-, keto-carboxylic acids and dicarbonyls. A series of dicarboxylic acids (C₂–C₂₄) were quantified. A detailed description of their individual abundances and discussion of interspecies relationships are already given in our previous paper (Li and Yu, 2010). Below is a brief account of the average values for the total concentrations and the few top abundant compounds in the three sample groups. The total concentrations were 740, 985, and 1374 ng m⁻³ during the local, cold front, and RT-influenced periods, respectively. Oxalic acid was the most abundant dicarboxylic acid, ranging from 539 to 882 ng m⁻³. Azelic acid (35.6–85.8 ng m⁻³), phthalic acid (33.8–77.9 ng m⁻³) and malonic acid (40.8–74.8 ng m⁻³) were the next three abundant dicarboxylic acid. Succinic acid (11.4–28.6 ng m⁻³), glutaric acid (6.9–21.3 ng m⁻³) and suberic acid (9.4–25.9 ng m⁻³) were the third abundant species (Figure S8f).

During local, cold front, and RT-influenced periods, the total concentrations of keto-carboxylic acids were 108, 171, and 245 ng m⁻³, while the total concentrations of dicarbonyls were 39, 93, and 123 ng m⁻³, respectively. Atmospheric production of dicarboxylic acids, ketocarboxylic acids and dicarbonyls through oxidation of hydrocarbon precursors is an important source for these compounds. The significant increases during cold front and RT-influenced periods indicated that more SOA formed during RT and LRT.

3.3. Source apportionment analysis of OC

CMB model is widely used to estimate the contributions of primary sources of OC and PM_{2.5} (Chow et al., 2007; Schauer et al., 1996; Schauer and Cass, 2000; Zheng et al., 2002, 2006). Most molecular markers and source profiles used in

CMB analysis were developed in the U.S. Multiple source profiles with speciated organics data have been published for important source classes such as motor vehicles, food cooking and wood combustion. It is not a trivial issue to select source profiles which can be used in local studies. Robinson et al. (2006a, 2006b, 2006c) and Subramanian et al. (2006) developed a new method to choose suitable markers and source profiles. The core part of this technique involves construction of plots of species concentrations (ratio–ratio plots, R–R plots) in which source profiles appear as points connected by linear mixing lines. This R–R plots technique is adopted here to facilitate the selection of source profiles and their respective characteristic tracers for vehicle exhaust, cooking, and road dust sources. After selecting source profiles and tracers, marker-to-OC ratios must be carefully considered because profiles with small marker-to-OC ratios will yield higher source contribution estimates than profiles with large ratios (Robinson et al., 2006c; Subramanian et al., 2006). Finally, Hong Kong local vehicle exhaust (Yu and Schauer, 2005), Hong Kong Daoxiang cooking (Yu et al., unpublished results) and Hong Kong road dust (Ho et al., 2003) met the requirement. Among them, the Hong Kong vehicle exhaust is derived from samples collected in a roadway tunnel in Hong Kong, without distinguishing diesel engine exhaust from gasoline-powered engine exhaust. Wherever possible, source profiles local to Hong Kong or specific to China were used in the CMB. The source profile of biomass burning is combined from burning emissions of cereal straw (including wheat, corn and rice), which is one of the most abundant biomass burned in China (Zhang et al., 2007), and six kinds of broad-leaf trees and shrubs in Southern China (Wang et al., 2009). Source profile of coal combustion is from Chinese industrial mixed coal : residential coal briquette = 1 : 3 (Zhang et al., 2008). The source profiles of vegetative detritus and cigarette smoke are obtained from the United States (Rogge et al., 1993a, 1994). Ship emission is from Canada (Lee and Kan, 2000). All these source profiles are plotted in Figure S9. The key tracer species used in CMB and their concentrations are listed in Table S1.

The CMB results are given in Table 2. Fig. 3 shows the bar charts of source distributions under different synoptic conditions. Figure S10 compares the measured and calculated concentrations of the tracers used in CMB model, using sample 040116 as an example. Figure S10 demonstrates that the calculated concentrations of all species are very close to the measured concentrations. The CMB analysis has identified vehicular exhaust to be the most important primary contributor to OC, accounting for 13.3–24.8% ($1.5\text{--}2.39\ \mu\text{g C m}^{-3}$) of fine OC. Biomass burning, coal combustion, and cooking were the next important sources, accounting for 3.6–9.8% ($0.31\text{--}1.62\ \mu\text{g C m}^{-3}$), 5.6–9.7% ($0.44\text{--}1.07\ \mu\text{g C m}^{-3}$), and 6.3–8.3% ($0.62\text{--}0.99\ \mu\text{g C m}^{-3}$) of fine OC, respectively. Suspended dust, cigarette smoke, ship emission, and vegetative detritus were minor sources, only contributing 0.44–1.07, 0.24–0.40, 0.21–0.28, 0.09–0.22, and 0.05–0.21 $\mu\text{g C m}^{-3}$, respectively.

During cold front periods, contributions of vehicle exhaust and ship emission were similar to those estimated for the local sample group, reflecting the dominance of local sources. In contrast, OC mass contributions from biomass burning and coal combustion in the LRT sample group almost triple and double, respectively, those in the local sample

group. This conclusion agrees with the much higher K^+/EC ratio and higher levoglucosan concentrations during the cold front and RT-influenced periods than during the local emissions-influenced periods. The highest contribution of coal combustion occurred during the cold-front periods, accounting for 9.7% of OC. This observation indicates that cold front brought extra coal combustion PM from outside PRD to Hong Kong. There was also increase in contribution to OC from suspended dust in the cold front LRT sample group.

The un-apportioned OC, also called “other OC”, is the difference between the measured OC and the apportioned primary OC by the CMB model, which consists of secondary OC as well as some unidentified primary sources. The amount of other OC was 3.84, 6.37, and 9.48 $\mu\text{g C m}^{-3}$ during local emissions-, cold front, and RT-influenced periods, respectively. Diacids are mainly of secondary origin and therefore part of SOA. Good correlation between other OC and diacids ($R^2 = 0.76$, $n = 21$, Figure S11) supports the other OC to be an approximate indicator for secondary OC. The elevated “other OC” level in the cold front and RT-influenced periods were consistent with the more aged air mass characteristics.

It is interesting to observe that the amount of OC apportioned to biomass burning was highly correlated to WSOC ($R^2 = 0.43$, $n = 21$) (Fig. 4). It has been reported that biomass burning particles contain a large amount of WSOC, accounting for 20.7–37.5% (Iinuma et al., 2007), 45–75% or even higher of OC (Graham et al., 2002; Mayol-Bracero et al., 2002). Work from our group also found biomass burning was the leading contributor to WSOC for particles in size bin of 1.0–1.8 μm collected in Shenzhen, a metropolitan city adjacent to Hong Kong (Huang et al., 2006). An examination of K^+ and sulfate revealed that the two were highly correlated ($R^2 = 0.52$, $n = 21$). The combined observations indicated that biomass burning emissions serve as significant precursors for secondary OC or the presence of biomass burning particles facilitates formation of SOA during RT and LRT.

3.4. Sensitivity test

The source profiles used in this study (Figure S9) are taken as the base case. When doing sensitivity test of a certain source, all the other source profiles in the base case remain unchanged. The source profile selections and sensitivity test results of cooking, vehicle exhaust, biomass burning and road dust are showed in Figure S12–S13. For coal combustion, the base case represents the medium contribution among industrial and residential coal combustions. The ratios between other cases and base case of cooking, vehicle exhaust, biomass burning, and coal combustion are almost within the 1:2 and 2:1 lines. As for road dust, Hong Kong local road dust had the highest estimated contribution than other cases, which resulted from its lowest Al/OC ratio. Although both dust source profiles from Rogge et al. (1993b) and Ho et al. (2003) had the similar R–R plot (Fe/Al vs. Ca/Al) as ambient samples, we used local road dust from Ho et al. (2003) study, since it is more representative of the Hong Kong condition.

4. Conclusions

In this study, 21 hi-volume $\text{PM}_{2.5}$ samples collected during January–March 2004 and January–March 2005 were classified

Table 2Source contributions to fine organic carbon ($\mu\text{g C m}^{-3}$).

Sample ID	Vehicle exhaust	Biomass burning	Cooking	Coal combustion	Road dust	Cigarette smoke	Ship emission	Vegetative detritus	Other OC ^a	Measured OC	%Mass ^b	R ²	χ^2
<i>Local emissions-dominated samples</i>													
040115	2.22 ± 0.33(24.7)	0.29 ± 0.09(3.2)	0.42 ± 0.11(4.6)	0.37 ± 0.06(4.1)	0.2 ± 0.04(2.3)	0.33 ± 0.06(3.6)	0.08 ± 0.02(0.9)	0.17 ± 0.07(1.8)	4.94(54.8)	9.02 ± 0.9	45.2	0.93	1.59
040131	1.23 ± 0.19(18.5)	0.09 ± 0.03(1.3)	0.66 ± 0.14(9.9)	0.11 ± 0.03(1.7)	0.15 ± 0.02(2.2)	0.18 ± 0.03(2.8)	0.11 ± 0.03(1.7)	0.04 ± 0.03(0.7)	4.05(61.2)	6.62 ± 0.66	38.8	0.95	1.09
040221	2.28 ± 0.34(30.2)	0.23 ± 0.07(3)	0.45 ± 0.12(5.9)	0.26 ± 0.05(3.5)	0.51 ± 0.08(6.8)	0.29 ± 0.06(3.8)	0.21 ± 0.05(2.7)	0.12 ± 0.06(1.5)	3.2(42.4)	7.54 ± 0.75	57.6	0.95	1.10
040229	1.01 ± 0.15(31.5)	0.01 ± 0.01(0.3)	0.2 ± 0.05(6.3)	0.04 ± 0.02(1.1)	0.16 ± 0.03(4.9)	0.06 ± 0.02(2)	0.16 ± 0.04(4.9)	0.01 ± 0.02(0.4)	1.55(48.6)	3.2 ± 0.32	51.4	0.94	1.14
040301	2.7 ± 0.51(33.1)	0.61 ± 0.18(7.5)	0.56 ± 0.17(6.9)	1.91 ± 0.23(23.5)	0.31 ± 0.05(3.8)	0.31 ± 0.05(3.8)	0.17 ± 0.05(2.1)	0 ± 0(0)	1.57(19.3)	8.14 ± 0.81	80.7	0.87	2.70
050228	1.55 ± 0.25(21.3)	0.39 ± 0.12(5.3)	1.41 ± 0.3(19.2)	0.38 ± 0.06(5.1)	0.16 ± 0.03(2.2)	0.12 ± 0.03(1.6)	0.09 ± 0.02(1.3)	0 ± 0(0)	3.2(43.8)	7.3 ± 0.73	56.2	0.92	1.48
050317	1.73 ± 0.26(14.5)	0.58 ± 0.17(4.9)	0.64 ± 0.16(5.4)	0.02 ± 0.03(0.2)	0.16 ± 0.03(1.3)	0.19 ± 0.04(1.6)	0.19 ± 0.04(1.6)	0.03 ± 0.04(0.2)	8.39(70.3)	11.93 ± 1.19	29.7	0.91	1.68
Avg.	1.82 ± 0.29(24.8)	0.31 ± 0.1(3.6)	0.62 ± 0.15(8.3)	0.44 ± 0.07(5.6)	0.24 ± 0.04(3.4)	0.21 ± 0.04(2.7)	0.14 ± 0.04(2.2)	0.05 ± 0.03(0.7)	3.84(48.7)	7.68 ± 0.77	51.3	0.93	1.54
<i>Samples influenced by cold front-long range transport</i>													
040113	1.94 ± 0.38(13.4)	1.06 ± 0.32(7.3)	0.66 ± 0.19(4.6)	1.39 ± 0.17(9.6)	0.34 ± 0.06(2.4)	0.31 ± 0.06(2.1)	0.08 ± 0.02(0.5)	0.29 ± 0.08(2)	8.36(58)	14.43 ± 1.44	42.0	0.93	1.56
040117	1.28 ± 0.22(13.5)	0.47 ± 0.14(4.9)	0.99 ± 0.23(10.4)	0.48 ± 0.07(5.1)	0.15 ± 0.03(1.5)	0.3 ± 0.06(3.2)	0.07 ± 0.02(0.8)	0.21 ± 0.07(2.2)	5.55(58.4)	9.51 ± 0.95	41.6	0.95	1.27
040121	0.69 ± 0.21(5.3)	1.42 ± 0.42(10.9)	0.26 ± 0.14(2)	1.06 ± 0.13(8.2)	0.83 ± 0.12(6.4)	0.19 ± 0.04(1.5)	0.09 ± 0.03(0.7)	0.12 ± 0.05(0.9)	8.32(64.1)	12.98 ± 1.3	35.9	0.94	1.24
040203	1.53 ± 0.31(18.2)	0.6 ± 0.18(7.1)	1.02 ± 0.24(12)	1.2 ± 0.15(14.2)	0.34 ± 0.05(4)	0.24 ± 0.05(2.9)	0.09 ± 0.02(1)	0.05 ± 0.04(0.6)	3.37(39.9)	8.43 ± 0.84	60.1	0.91	1.97
040303	1.52 ± 0.34(16.5)	0.59 ± 0.18(6.4)	0.58 ± 0.17(6.2)	1.79 ± 0.21(19.3)	0.55 ± 0.08(5.9)	0.22 ± 0.05(2.4)	0.1 ± 0.03(1.1)	0.11 ± 0.06(1.2)	3.77(40.8)	9.23 ± 0.92	59.2	0.92	1.76
050131	1.72 ± 0.31(14.1)	1.16 ± 0.34(9.5)	1.23 ± 0.29(10.1)	0.74 ± 0.11(6)	0.24 ± 0.04(2)	0.15 ± 0.04(1.2)	0.15 ± 0.04(1.2)	0.05 ± 0.04(0.4)	6.78(55.5)	12.21 ± 1.22	44.5	0.91	1.92
050220	1.84 ± 0.34(12.4)	1.58 ± 0.46(10.6)	1.54 ± 0.36(10.3)	0.85 ± 0.13(5.7)	0.35 ± 0.05(2.4)	0.16 ± 0.04(1.1)	0.08 ± 0.02(0.6)	0.08 ± 0.05(0.5)	8.43(56.5)	14.9 ± 1.49	43.5	0.91	1.94
Avg.	1.5 ± 0.3(13.3)	0.98 ± 0.29(8.1)	0.9 ± 0.23(8)	1.07 ± 0.14(9.7)	0.4 ± 0.06(3.5)	0.22 ± 0.05(2)	0.09 ± 0.03(0.8)	0.13 ± 0.06(1.1)	6.37(53.3)	11.67 ± 1.17	46.7	0.92	1.67
<i>Samples influenced by regional transport from PRD</i>													
040111	2.16 ± 0.42(14.5)	0.61 ± 0.19(4.1)	1.67 ± 0.38(11.2)	1.45 ± 0.18(9.7)	0.33 ± 0.06(2.2)	0.31 ± 0.06(2.1)	0.15 ± 0.04(1)	0.19 ± 0.07(1.3)	8.03(53.9)	14.9 ± 1.49	46.1	0.94	1.42
040116	2.32 ± 0.46(19.3)	1.14 ± 0.34(9.5)	0.82 ± 0.22(6.8)	1.77 ± 0.21(14.7)	0.25 ± 0.05(2.1)	0.24 ± 0.05(2)	0.17 ± 0.04(1.4)	0.27 ± 0.08(2.2)	5.07(42)	12.05 ± 1.21	58.0	0.97	0.77
040130	3.01 ± 0.58(12)	1.35 ± 0.41(5.4)	0.89 ± 0.27(3.5)	2.01 ± 0.26(8)	0.56 ± 0.1(2.2)	0.42 ± 0.08(1.7)	0.38 ± 0.09(1.5)	0.42 ± 0.12(1.7)	16(63.9)	25.03 ± 2.5	36.1	0.94	1.44
040222	1.62 ± 0.31(8.4)	1.79 ± 0.56(9.3)	0.44 ± 0.19(2.3)	0.78 ± 0.11(4)	0.49 ± 0.08(2.5)	0.34 ± 0.07(1.8)	0.15 ± 0.04(0.8)	0.4 ± 0.1(2.1)	13.2(68.7)	19.2 ± 1.92	31.3	0.94	1.40
050204	2.14 ± 0.31(18.4)	0.65 ± 0.19(5.6)	0.72 ± 0.18(6.2)	0.07 ± 0.04(0.6)	0.16 ± 0.03(1.4)	0.21 ± 0.04(1.8)	0.16 ± 0.04(1.4)	0.04 ± 0.04(0.3)	7.44(64.2)	11.59 ± 1.16	35.8	0.92	1.61
050222	3.21 ± 0.51(19)	2.28 ± 0.66(13.4)	1.52 ± 0.38(9)	0.49 ± 0.12(2.9)	0.24 ± 0.04(1.4)	0.23 ± 0.06(1.4)	0.26 ± 0.07(1.6)	0 ± 0.06(0)	8.71(51.4)	16.95 ± 1.69	48.6	0.91	1.80
050305	2.3 ± 0.41(14.2)	3.5 ± 1.04(21.6)	0.85 ± 0.31(5.2)	0.56 ± 0.12(3.5)	0.44 ± 0.07(2.7)	0.21 ± 0.06(1.3)	0.3 ± 0.08(1.9)	0.12 ± 0.07(0.7)	7.93(48.9)	16.22 ± 1.62	51.1	0.91	1.80
Avg.	2.39 ± 0.43(15.1)	1.62 ± 0.48(9.8)	0.99 ± 0.28(6.3)	1.02 ± 0.15(6.2)	0.35 ± 0.06(2.1)	0.28 ± 0.06(1.7)	0.22 ± 0.06(1.4)	0.21 ± 0.08(1.2)	9.48(56.2)	16.56 ± 1.66	43.8	0.93	1.46

The value in parentheses is the contribution percentage of each source to fine OC.

^a Other OC is the difference between measured OC and calculated primary OC.^b %Mass means the sum percentage of estimated primary source contributions in total measured fine OC.

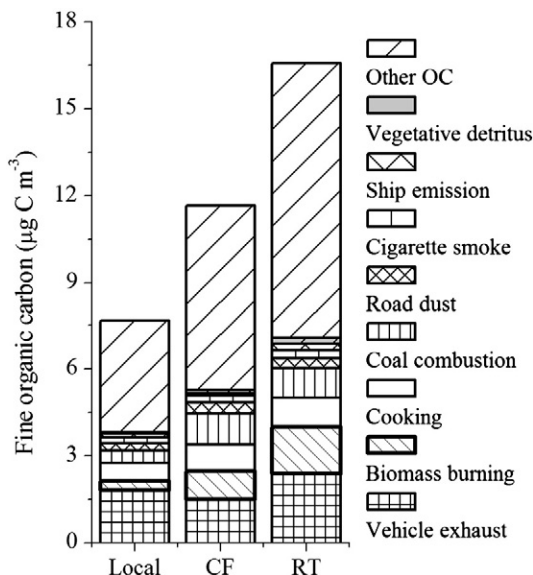


Fig. 3. Source contributions to fine organic carbon under different meteorological conditions. (CF: cold front long range transport; RT: regional transport from PRD).

into three groups according to meteorological conditions and criteria air pollutant data. The groups are local emissions-dominated samples, cold front LRT-influenced samples, and PRD RT-dominated samples. During the cold front periods, the levels of $PM_{2.5}$ and its major constituents were within the range of those collected in the local emissions-dominated and RT-dominated samples. However, the highest K^+/EC and OC/EC ratios and the lowest EC concentration occurred during cold front episodes. Source analysis by CMB model indicates that vehicle exhaust of mainly local origin was a major source of OC in all types of samples. When air masses were transported from the PRD region or beyond the PRD, contributions by biomass burning and coal combustion increased. A more prominent difference of the cold front periods and the RT-dominated periods relative to the local emissions-dominated period was

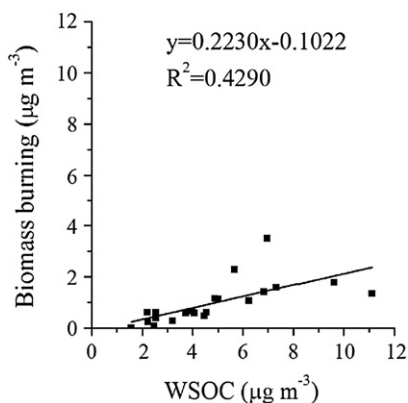


Fig. 4. Scatter plot of OC attributable to biomass burning versus $WSOC$.

significant increases in the amount of unexplained OC (or other OC). Other OC was shown to be mainly of secondary origin. Source analysis as well as tracer concentration variation indicate that biomass burning OC and $WSOC$ were correlated.

Acknowledgments

This work was supported by the Research Grants Council of Hong Kong, China (602103 and 605404) and the Hong Kong Environment Protection Department.

Appendix A. Supplementary data

Supplementary data to this article can be found online at <http://dx.doi.org/10.1016/j.atmosres.2012.05.026>.

References

- Birch, M.E., Cary, R.A., 1996. Elemental carbon-based method for monitoring occupational exposures to particulate diesel exhaust. *Aerosol. Sci. Technol.* 25, 221–241.
- Cass, G.R., 1998. Organic molecular tracers for particulate air pollution sources. *Trends Anal. Chem.* 17, 356–366.
- Chow, J.C., Watson, J.G., Lowenthal, D.H., Chen, L.W.A., Zielinska, B., Mazzoleni, L.R., Magliano, K.L., 2007. Evaluation of organic markers for chemical mass balance source apportionment at the Fresno Supersite. *Atmos. Chem. Phys.* 7 (7), 1741–1754.
- Fang, M., Zheng, M., Wang, F., Chim, K.S., Kot, S.C., 1999. The long-range transport of aerosols from northern China to Hong Kong – a multi-technique study. *Atmos. Environ.* 33, 1803–1817.
- Fung, J.C.H., Lau, A.K.H., Lam, J.S.L., Yuan, Z., 2005. Observational and modeling analysis of a severe air pollution episode in western Hong Kong. *J. Geophys. Res.* 110, D09105, <http://dx.doi.org/10.1029/2004JD005105>.
- Gelencser, A., 2004. *Carbonaceous Aerosol. : Atmospheric and Oceanographic Sciences Library*, vol. 30. Springer.
- Graham, B., Mayol-Bracero, O.L., Guyon, P., Roberts, G.C., Decesari, S., Facchini, M.C., et al., 2002. Water-soluble organic compounds in biomass burning aerosols over Amazonia I. Characterization by NMR and GC-MS. *J. Geophys. Res.* 107 (D20), 8047, <http://dx.doi.org/10.1029/2001JD000336>.
- Hagler, G.S.W., Bergin, M.H., Salmon, L.G., Yu, J.Z., Wan, E.C.H., Zheng, M., Zeng, L.M., Kiang, C.S., Zhang, Y.H., Schauer, J.J., 2007. Local and regional anthropogenic influence on $PM_{2.5}$ elements in Hong Kong. *Atmos. Environ.* 41 (28), 5994–6004.
- Ho, S.S.H., Yu, J.Z., 2004. In-injection port thermal desorption and subsequent gas chromatography–mass spectrometric analysis of polycyclic aromatic hydrocarbons and n-alkanes in atmospheric aerosol samples. *J. Chromatogr. A* 1059, 121–129.
- Ho, K.F., Lee, S.C., Chow, J.C., Watson, J.G., 2003. Characterization of PM_{10} and $PM_{2.5}$ source profiles for fugitive dust in Hong Kong. *Atmos. Environ.* 37, 1023–1032.
- Ho, K.F., Lee, S.C., Cao, J.J., Chow, J.C., Watson, J.G., Chan, C.K., 2006. Seasonal variations and mass closure analysis of particulate matter in Hong Kong. *Sci. Total. Environ.* 355, 276–287.
- Ho, S.S.H., Yu, J.Z., Chow, J.C.J., Watson, G., Zielinska, B., Watson, J.G., Sit, E.H.L., Schauer, J.J., 2008. Evaluation of an in-injection port thermal desorption gc-ms method for analysis of non-polar organic compounds in ambient aerosol samples. *J. Chromatogr. A* 1200 (2), 217–227.
- Ho, S.S.H., Chow, J.C., Watson, J.G., Ng, L.P.T., Kwok, Y., Ho, K.F., Cao, J.J., 2011. Precautions in application of injection port-thermal desorption/mass spectrometry (TD-GC/MS) in analysis of aerosol loaded filters. *Atmos. Environ.* 45, 1491–1496.
- Huang, X.F., Yu, J.Z., He, L.Y., Yuan, Z.B., 2006. Water-soluble organic carbon and oxalate in aerosol at a coastal urban site in China, size distribution characteristics, sources, and formation mechanisms. *J. Geophys. Res.* 111, D22212, <http://dx.doi.org/10.1029/2006JD007408>.
- Huang, H., Ho, K.F., Lee, S.C., Tsang, P.K., Ho, S.S.H., Zou, C.W., Cao, J.J., Xu, H.M., 2012. Characteristics of carbonaceous aerosol in $PM_{2.5}$: Pearl Delta River Region, China. *Atmos. Res.* 104–105, 227–236.
- Iinuma, Y., Brüeggemann, E., Gnauk, T., Mueller, K., Andreae, M.O., Helas, G., Parmar, R., Herrmann, H., 2007. Source characterization of biomass burning particles: the combustion of selected European conifers, African hardwood, savanna grass, and German and Indonesian peat. *J. Geophys. Res.* 112 (D8) Art. No. D08209.

- Lau, A.K.H., Lo, A., Gray, J., Yuan, Z.B., Loh, C., 2007. Relative significance of local vs. regional sources: Hong Kong's air pollution. March Civic Exchange, Environment and Conservation. http://www.civic-exchange.org/eng/upload/files/200703_HKAirPollution.pdf.
- Lee, Y.C., Hills, P.R., 2003. Cool season pollution episodes in Hong Kong, 1996–2002. *Atmos. Environ.* 37, 2927–2939.
- Lee, S.W., Kan, R.P.B., 2000. A new methodology for source characterization of oil combustion particulate matter. *Fuel Process. Technol.* 65–66, 189–202.
- Li, Y.C., 2008. Characterization of polar organic compounds and source analysis of fine organic aerosols in Hong Kong. The Hong Kong University of Science and Technology, PhD thesis.
- Li, Y.C., Yu, J.Z., 2005. Simultaneous determination of mono- and dicarboxylic acids, omega-oxo-carboxylic acids, midchain ketocarboxylic acids, and aldehydes in atmospheric aerosol samples. *Environ. Sci. Technol.* 39 (19), 7616–7624.
- Li, Y.C., Yu, J.Z., 2010. Composition profile of oxygenated organic compounds and inorganic ions in PM_{2.5} in Hong Kong. *Environ. Chem.* 7, 338–349.
- Lin, P., Engling, G., Yu, J.Z., 2010. Humic-like substances in fresh emissions of rice straw burning and in ambient aerosols in the Pearl River Delta Region, China. *Atmos. Chem. Phys.* 10, 6487–6500.
- Liu, H.P., Chan, J.C.L., 2002. An investigation of air-pollutant patterns under sea-land breezes during a severe air-pollution episode in Hong Kong. *Atmos. Environ.* 36, 591–601.
- Lo, J.C.F., Lau, A.K.H., Fung, J.C.H., Chen, F., 2006. Investigation of enhanced cross-city transport and trapping of air pollutants by coastal and urban land-sea breeze circulations. *J. Geophys. Res. Atmos.* 111 (D14) Art. No. D14104.
- Louie, P.K.K., Watson, J.G., Chow, J.C., Chen, A., Sin, D.W.M., Lau, A.K.H., 2005. Seasonal characteristics and regional transport of PM_{2.5} in Hong Kong. *Atmos. Environ.* 39, 1695–1710.
- Mayol-Bracero, O.L., Guyon, P., Graham, B., Roberts, G., Andreae, M.O., Decesari, S., Facchini, M.C., Fuzzi, S., Artaxo, P., 2002. Water-soluble organic compounds in biomass burning aerosols over Amazonia—2. Apportionment of the chemical composition and importance of the polyacidic fraction. *J. Geophys. Res. Atmos.* 107 (D20) Art. No. 8091.
- Medeiros, P.M., Simoneit, B.R.T., 2007. Analysis of sugar in environmental samples by gas chromatography–mass spectrometry. *J. Chromatogr. A* 1141, 271–278.
- Peters, A., Liu, E., Verrier, R.L., Schwartz, J., et al., 2000. Air pollution and incidence of cardiac arrhythmia. *Epidemiology* 11, 11–17.
- Pope, C.A., 2000a. Review, epidemiological basis for particulate air pollution health standards. *Aerosol. Sci. Technol.* 32 (1), 4–14.
- Pope, C.A., 2000b. What do epidemiologic findings tell us about health effects of environmental aerosols? *J. Aerosol. Med. Pulm. D* 13 (4), 335–354.
- Robinson, A.L., Subramanian, R., Donahue, N.M., Bernardo-Bricker, A., Rogge, W.F., 2006a. Source apportionment of molecular markers and organic aerosols-1. Polycyclic aromatic hydrocarbons and methodology for data visualization. *Environ. Sci. Technol.* 40 (24), 7803–7810.
- Robinson, A.L., Subramanian, R., Donahue, N.M., Bernardo-Bricker, A., Rogge, W.F., 2006b. Source apportionment of molecular markers and organic aerosol. 2. Biomass smoke. *Environ. Sci. Technol.* 40 (24), 7811–7819.
- Robinson, A.L., Subramanian, R., Donahue, N.M., Bernardo-Bricker, A., Rogge, W.F., 2006c. Source apportionment of molecular markers and organic aerosol. 3. Food cooking emissions. *Environ. Sci. Technol.* 40 (24), 7820–7827.
- Rogge, W.F., Hildemann, L.M., Mazurek, M.A., Cass, G.R., Simoneit, B.R.T., 1991. Sources of fine organic aerosol. 1. Charbroilers and meat cooking operations. *Environ. Sci. Technol.* 25, 1112–1125.
- Rogge, W.F., Hildemann, L.M., Mazurek, M.A., Cass, G.R., Simoneit, B.R.T., 1993a. Sources of fine organic aerosol. 4. Particulate abrasion products from leaf surfaces of urban plants. *Environ. Sci. Technol.* 27, 2700–2711.
- Rogge, W.F., Hildemann, L.M., Mazurek, M.A., Cass, G.R., Simoneit, B.R.T., 1993b. Source of fine organic aerosol. 3. Road dust, tire debris, and organometallic brake lining dust, roads as sources and sinks. *Environ. Sci. Technol.* 27, 1892–1904.
- Rogge, W.F., Hildemann, L.M., Mazurek, M.A., Cass, G.R., Simoneit, B.R.T., 1994. Sources of fine organic aerosol. 6. Cigarette smoke in the urban atmosphere. *Environ. Sci. Technol.* 28, 1375–1388.
- Schauer, J.J., Cass, G.R., 2000. Source apportionment of wintertime gas-phase and particle-phase air pollutants using organic compounds as tracers. *Environ. Sci. Technol.* 34 (9), 1821–1832.
- Schauer, J.J., Rogge, W.F., Hildemann, L.M., Mazurek, M.A., Cass, G.R., Simoneit, B.R.T., 1996. Source apportionment of airborne particulate matter using organic compounds as tracers. *Atmos. Environ.* 30, 3837–3855.
- Schwartz, J., Dochery, D.W., Neas, L.M., 1996. Is daily mortality associated specifically with fine particles? *J. Air Waste Manage.* 46, 2–14.
- Simoneit, B.R.T., Elias, V.O., Kobayashi, M., Kawamura, K., Rushdi, A.I., et al., 2004. Sugars—dominant water-soluble organic compounds in soils and characterization as tracers in atmospheric particulate matter. *Environ. Sci. Technol.* 38, 5939–5949.
- Subramanian, R., Donahue, N.M., Bernardo-Bricker, A., Rogge, W.F., Robinson, A.L., 2006. Contribution of motor vehicle emissions to organic carbon and fine particle mass in Pittsburgh, Pennsylvania: effects of varying source profiles and seasonal trends in ambient marker concentrations. *Atmos. Environ.* 40 (40), 8002–8019.
- Swami, K., Judd, C.D., Orsini, J., Yang, K.X., Husain, L., 2001. Microwave assisted digestion of atmospheric aerosol samples followed by inductively coupled plasma mass spectrometry determination of trace elements. *Fresen. J. Anal. Chem.* 369, 63–70.
- Tan, J.H., Guo, S.J., Ma, Y.L., Duan, J.C., Cheng, Y., He, K.B., Yang, F.M., 2011. Characteristics of particulate PAHs during a typical haze episode in Guangzhou, China. *Atmos. Res.* 102, 91–98.
- Turpin, B.J., Lim, H.J., 2001. Species contributions to PM_{2.5} mass concentrations: Revising common assumptions for estimating organic mass. *Aerosol Sci. Tech.* 35, 602–610.
- Wai, K.M., Tanner, P.A., 2005. Extreme particulate levels at a western pacific coastal city: the influence of meteorological factors and the contribution of long-range transport. *J. Atmos. Chem.* 50 (2), 103–120.
- Wang, T.J., Lam, K.S., Xie, M., Wang, X.M., Carmichael, G., Li, Y.S., 2006. Integrated studies of a photochemical smog episode in Hong Kong and regional transport in the Pearl River Delta of China. *Tellus* 58B, 31–40.
- Wang, Z.Z., Bi, X.H., Sheng, G.Y., Fu, J.M., 2009. Characterization of organic compounds and molecular tracers from biomass burning smoke in South China I: broad-leaf trees and shrubs. *Atmos. Environ.* 43, 3096–3102.
- Weast, R.C. (Ed.), 1988. *CRC Handbook of Chemistry and Physics*, First Student Edition. CRC Press, Inc., Boca Raton, Florida.
- Yang, H., Li, Q.F., Yu, J.Z., 2003. Comparison of two methods for the determination of water-soluble organic carbon in atmospheric particles. *Atmos. Environ.* 37, 865–870.
- Yang, H., Yu, J.Z., Ho, S.S.H., Xu, J.H., Wu, W.-S., Wan, C.H., Wang, X.D., Wang, X.R., Wang, L.S., 2005. The chemical composition of inorganic and carbonaceous materials in PM_{2.5} in Nanjing, China. *Atmos. Environ.* 39 (20), 3735–3749.
- Yu, J.Z., Schauer, J.J., 2005. Chemical characterization of water soluble organic compounds in particulate matters in Hong Kong. Final Report Submitted to the HKEPD, AS 03–399.
- Yu, J.Z., Tung, J.W.T., Wu, A.W.M., Lau, A.K.H., Louie, P.K.K., Fung, J.C.H., 2004. Abundance and seasonal characteristics of elemental and organic carbon in Hong Kong. *Atmos. Environ.* 38, 1511–1521.
- Yu, J.Z., Huang, X.H.H., Ho, S.S.H., Bian, Q.J., 2011. Nonpolar organic compounds in fine particles: quantification by thermal desorption-GC/MS and evidence for their significant oxidation in ambient aerosols in Hong Kong. *Anal. Bioanal. Chem.* 401, 3125–3139.
- Yuan, Z.B., Lau, A.K.H., Zhang, H.Y., Yu, J.Z., Louie, P.K.K., Fung, J.C.H., 2006. Identification and spatiotemporal variations of dominant PM₁₀ sources over Hong Kong. *Atmos. Environ.* 40, 1803–1815.
- Zhang, Y.X., Shao, M., Zhang, Y.H., Zeng, L.M., He, L.Y., Zhu, B., Wei, Y.J., Zhu, X.L., 2007. Source profiles of particulate organic matters emitted from cereal straw burnings. *J. Environ. Sci.* 19, 167–175.
- Zhang, Y.X., Schauer, J.J., Zhang, Y.H., Zeng, L.M., Wei, Y.J., Liu, Y., Shao, M., 2008. Characteristics of particulate carbon emissions from real-world Chinese coal combustion. *Environ. Sci. Technol.* 42, 5068–5073.
- Zheng, M., Cass, G.R., Schauer, J.J., Edgerton, E.S., 2002. Source apportionment of PM_{2.5} in the Southeastern United States using solvent-extractable organic compounds as tracers. *Environ. Sci. Technol.* 36, 2361–2371.
- Zheng, M., Hagler, G.S.W., Ke, L., Bergin, M.H., Wang, F., Louie, P.K.K., Salmon, Y., Sin, D.W.M., Yu, J.Z., Schauer, J.J., 2006. Composition and sources of carbonaceous aerosols at three contrasting sites in Hong Kong. *J. Geophys. Res.* 111, D20313. <http://dx.doi.org/10.1029/2006JD007074>.